MISR: A New Way to Look at Clouds

L. Di Girolamo[1], E.E. Clothiaux[2], R. Davies[3], D.J. Diner[4], C. Moroney[3], J.-P. Muller[5], T. Varnai[6], and G. Zhao[1]

[1]Department of Atmospheric Sciences, University of Illinois, Urbana, IL 61801-3070
[2]Department of Meteorology, Pennsylvania State University, University Park, PA 16802
[3]Institute of Atmospheric Physics, University of Arizona, Tucson, AZ 85721-0081
[4]Jet Propulsion Laboratory, MS 169-237, Pasadena, CA 91109-8099
[5]Department of Geomatic Engineering, University College London, UK
[6]Goddard Space Flight Center, MS 913, Greenbelt, MD 20771

INTRODUCTION

The Multi-angle Imaging SpectroRadiometer (MISR) on-board EOS-Terra is the first high-resolution imager to make global, near-simultaneous, multi-spectral, multi-angle radiometric measurements of the Earth (Diner *et al.* 1998). Its unique ability to retrieve combined spectral and angular signatures allows us to exploit both the spectral and angular information content of the upwelling radiation field in order to remotely sense properties of the Earth-atmosphere system. This paper highlights two of MISR's unique ways of studying clouds: (1) a stereoscopic capability to derive cloud-top heights and to detect cloud, and (2) the first application of band-differenced angular signatures to detect thin cirrus clouds.

STEREO

MISR can determine cloud motion and cloud-top heights by matching up common features in images viewed at different angles. The observed "shift" or disparities can be combined with the viewing geometry and converted into motion or height values. (Diner *et al.*1999). Examples of the MISR area-matchers used in determining cloud-top height follow. Area-matchers work by stepping a small patch of pixels in one image through a search window in the second image and finding the locations where the difference metric between the two patches is minimized. For operational processing, MISR determines the cloud-top heights independently using the forward and aft views, and rejecting those points where the difference between the two heights lies a given distance away from the mean.

An estimate of the stereo height uncertainty can be determined under clear skies by comparing the stereo height field to the known surface elevation. On a limited set of scenes analyzed thus far, the average error was 130 m with a standard deviation of 500 m, which is equal to the minimum height resolution using the 26.5° fore and aft camera views for matching. Once independent cloud-top height information becomes available, the error in stereo cloud-top heights can be ascertained; however, similar errors as derived for surface elevation are expected.

Figure 1 shows a sample image of a partly cloudy scene for the nadir camera and the resulting along-track disparity field from stereo. Height fields are not presented because accurate geometrical calibration, which is required to correct for the disparity caused by cloud motion, is pending at the time of publication. From Fig. 1, it is evident that stereo retrieves both broad and fine scale features. The various cloud layers at different elevations show up clearly as regions with different disparities, and features that span only a few pixels are also detected. Note, in the upper right corner and bottom of Fig. 1b, stereo was able to retrieve the presence of some very thin cirrus clouds that cannot be seen in Fig. 1b using the current color table. The magnitudes of the retrieved disparities match up well with those obtained by manually matching different areas of the images.

Stereo also provides a simple test for cloud detection: if the retrieved stereo height for a pixel is greater than the known surface elevation plus the uncertainty in the height, then the pixel is labeled cloudy. Since stereo is independent of spectral signatures, this technique becomes a powerful cloud detection technique over traditionally difficult surfaces (e.g., snow, desert).

BAND DIFFERENCED ANGULAR SIGNATURES

Di Girolamo and Davies (1994) developed a Band Differenced Angular Signature (BDAS) technique for high cloud detection based on radiative transfer simulations. The BDAS technique takes the difference between MISR's 0.44 μm and 0.86 μm reflectance and examines this difference as a function of view angle. The resulting signature is sensitive to the contribution of Rayleigh scattering to the total reflectance. Since this contribution changes in the presence of clouds, especially high clouds, the BDAS can be used to differentiate high clouds from low clouds and clear sky. Empirical proof of the BDAS technique is now feasible using MISR data.

Figure 2a is the nadir camera 0.86 μm image acquired on March 2, 2000 over the South Atlantic. The scene is characterized by a mix of high and low clouds, clear ocean scenes, and an iceberg measuring approximately 66 km long. Figure 3 shows the 0.44 – 0.86 μm reflectance difference as a function of MISR view angle for a variety of scenes taken from Fig. 2a. In choosing these scenes, it is assumed that visual inspection provides the correct scene classification. Note that the clear and cloudy scenes have the largest slope differences in the most oblique cameras that view the forward scattered radiation. For this reason, the MISR cloud detection algorithm constructs a BDAS proportional to

Figure 1. (a) A MISR red-channel image acquired on February 25, 2000 over the South Pacific; (b) The MISR stereo disparity field for image (a). In (b), black represents low and white high disparity.

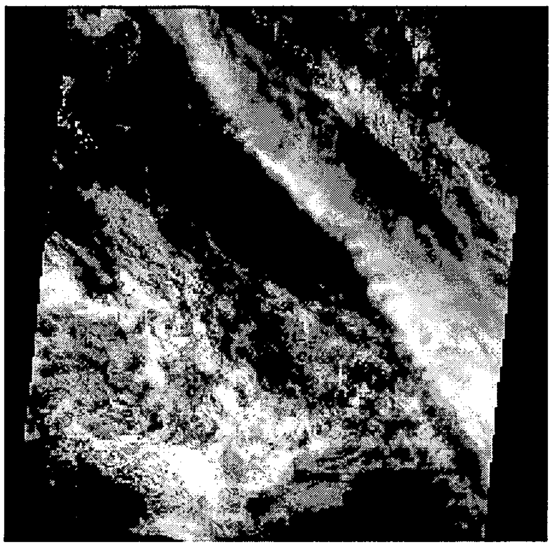

(a)

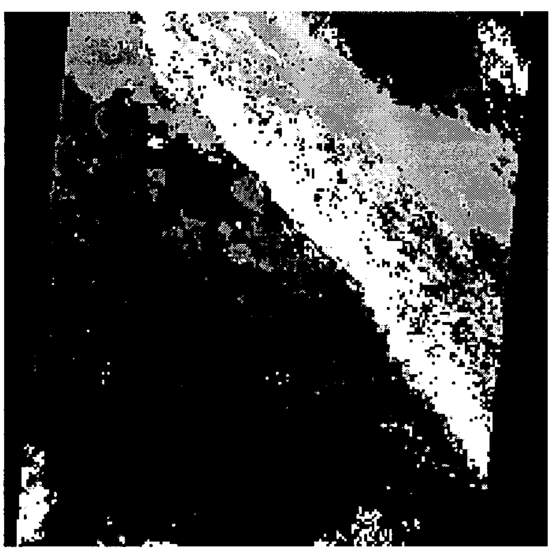

(b)

$$BDAS \propto (R^{70.5}_{0.44} - R^{70.5}_{0.86}) - (R^{60}_{0.44} - R^{60}_{0.86})$$

where R^{θ}_{x} is the bidirectional reflectance factor of spectral channel x, viewing the forward scattered radiation in direction θ. Figure 2b shows the BDAS image corresponding to Fig. 2a. Note, the thin cirrus over the ocean (to the west of the iceberg) is apparent in Fig. 2b and not in Fig. 2a. Even over the iceberg, contrast exists in Fig. 2b between the thin cloud over the north-central area of the iceberg and the surrounding clear sky area. This is not the case in Fig. 2a. The contrast between clear-sky ocean and ice is as expected based on Di Girolamo and Davies (1994).

FUTURE WORK

This paper has presented some examples of how MISR can employ its unique multi-angle viewing capability to retrieve cloud-top height and provide novel techniques to perform cloud detection. In addition, MISR will also be able to retrieve better estimates of cloud albedo compared to single-view instruments. Most instruments used to derive a global albedo data set can only view a particular scene once during its orbit. As a result, the albedo for the scene is estimated based on one radiance value from a particular direction. However, MISR can make radiance measurements of the same scene at nine different view-angles, essentially providing a cross-section in view-zenith of the upwelling radiance field. Varnai (1996) performed theoretical calculations demonstrating reduced cloud albedo uncertainty using the MISR albedo algorithm compared to a single-view algorithm. At the time of publication, the MISR albedo product has not been examined, since this requires accurate stereo heights and radiometric calibration, and validation data from in situ measurements. However, the MISR albedo algorithm was successfully applied to AirMISR data (Varnai *et al.* 1999). Future work will concentrate on validating the radiometric and geometric calibration and the standard operational algorithms currently in place to analyze the MISR data.

ACKNOWLEDGMENTS

Support from NASA's Earth Observing System Program is gratefully acknowledged.